RSC Advances

PAPER

View Article Online
View Journal | View Issue

Cite this: *RSC Adv.*, 2015, **5**, 61554

Improving the tribological properties of NiAl matrix composites *via* hybrid lubricants of silver and graphene nano platelets

Ahmed Mohamed Mahmoud Ibrahim,[ab] Xiaoliang Shi,*[a] Wenzheng Zhai[a] and Kang Yang[a]

Received 19th June 2015
Accepted 10th July 2015

DOI: 10.1039/c5ra11862j

www.rsc.org/advances

This work presents a comprehensive study of the synergistic tribological effect of combined solid lubricants of silver and graphene nano platelets (GNPs). Moreover, it presents a comparative study of the tribological characteristics of NiAl (NA), NiAl-10 wt% silver (NAS), NiAl-1.5 wt% GNPs (NAG), NiAl-1.5 wt% GNPs-10 wt% silver (NAGS10) and NiAl-1.5 wt% GNPs-15 wt% silver (NAGS15) composites based on tribological and microstructural tests. The NAGS10 composite shows the lowest friction coefficients and the highest wear resistance among the whole composites at different sliding velocities and applied loads, while NA exhibits the highest friction coefficients and wear rates at the same sliding conditions. The microstructural tests of NAGS10 and NAGS15 composites reveal the formation of GNPs and silver enriched islands which act as the bearing areas and play the major role in loading transition. Furthermore, those islands ease the slipping of the graphene layers over the NiAl substrate.

1. Introduction

NiAl has relatively low density, high strength, high melting point, high thermal conductivity and excellent oxidation resistance. Due to these attractive characteristics, NiAl becomes a good candidate for producing gas turbine engines for aircraft, electronic metallization compounds in advanced semiconductors, heterostructures and surface catalysts, among many others.[1–3]

Improving the frictional properties and the wear resistance of NiAl composites is a challenge. Recently, many efforts have been done to improve the tribological characteristics of NiAl composites at different conditions *via* composing the solid lubricants into the composites. Graphite has been frequently used as a solid lubricant and it has been composed in many composites to improve the tribological properties of these composites at different sliding conditions. It is reported that adding Ni-coated graphite with 8 wt% to aluminum composites is able to decrease the wear rates and the friction coefficient to about 0.35. Furthermore, graphite has superior lubrication effect if compared to h-BN.[4,5] Besides, metal matrix–graphite particle composites exhibited lower friction coefficients and wear rates compared with graphite free composites.[6]

Graphene is proposed as a promising material which has a reinforcement and lubrication effects due to the easy shear capabilities, smooth atomic surface and the extreme strength in addition of the distinction optical, electrical properties, chemical resistance and thermal stability.[7–11] Furthermore, graphene single layer showed lower friction coefficients and higher wear resistance than the graphite at the same sliding conditions.[12] Zhai *et al.*[13] proved that a small amount of graphene nano platelets is able to improve the tribological properties of Ni_3Al composites. Moreover, adding 1.5 wt% graphene is a good approach to decrease the friction coefficients and the wear rates of NiAl composites under different sliding velocities.[1] Furthermore, it is stated that graphene could increase the wear resistance of polyethylene composites by more than four times.[14] It is also concluded that adding 1 wt% multi-layer graphene increases the hardness and the elastic modulus besides the improvement of the tribological properties of Ni_3Al composites.[15] Yang *et al.* proved that multi-layer graphene can improve the tribological characteristics of TiAl matrix composites at different loads lower than 12 N.[16]

Another material, which exhibits good tribological characteristics at a wide range of temperature, is silver. Silver has been used as a solid lubricant due to low shear conjunctions. The tribological properties of either only the silver or with other solid lubricants have been extensively studied by many researchers in the last decades. It is stated that adding the silver to NiCr–Cr_2O_3 could decrease the friction coefficient significantly.[17] Tyagi *et al.* proved that adding silver and hBN is an effective mean to reduce the friction coefficient and to improve

[a]*School of Mechanical and Electronic Engineering, Wuhan University of Technology, 122 Luoshi Road, Wuhan 430070, China. E-mail: sxl071932@126.com; Fax: +86-27-87651793; Tel: +86-27-87651793*

[b]*Production Engineering and Design Department, Faculty of Engineering, Minia University, El Minia 61111, Egypt*

the wear resistance of Ni based composites at elevated temperatures, different loads and different sliding speeds. Besides, it is reported that silver could reduce the friction coefficient of Ni-based composites from 0.36 to 0.21 at high loads and high sliding speeds.[18,19]

The synergistic effect of silver and molybdenum disulfide has been investigated.[20] It is reported that using silver and molybdenum disulfide with contents of 20 wt% and 8 wt% respectively decreased the friction coefficient and the wear rate of Ni based self-lubricating composites at different conditions. Moreover, TiB_2 and silver play the major role in improving the wear resistance and decreasing the friction coefficient of the TiAl composites.[21] Shi *et al.*[22] investigated the tribological effect of using Ag, Ti_3SiC_2 and eutectic (BaF_2-38 wt% CaF_2) solid lubricants mixture. The results revealed that the tribological properties have been improved through adding the Ag, Ti_3SiC_2 and eutectic (BaF_2-38 wt% CaF_2) mixture at elevated temperatures. Moreover, using silver with barium salts ($BaCrO_4$ and $BaMoO_4$) is an effective way to decrease the friction coefficients of Ni_3Al composites at temperature of 800 °C.[23]

Until now, the synergistic effect of Ag and graphene nano platelets has not been investigated. Therefore, this study has been done to investigate the enhancement and the tribological effect of using GNPs and Ag on NiAl matrix composites at different loads and sliding speeds.

2. Experimental procedure

2.1 Material preparing and characterization

The composite powders of NiAl matrix were composed of commercially available Ni, Al, Mo, Nb, B and Cr powders (30–50 μm in average size, 99.9 wt% in purity) by weight fractions 64, 30, 2, 1.5, 0.5 and 2%. Graphene nano platelets powder (lateral size of 0.5–5 μm and average thickness of 40 nm) was added with a weight fraction of 1.5% while the weight fractions of silver powder (20–40 μm) were 10 and 15%. The graphene nano platelet powder was purchased from Nanjing XFNANO Materials Tech Co., Ltd. The powders were mechanically mixed using polytetrafluoroethylene (PTFE) vials and 45 Hz of vibrating frequency. After that, the NiAl matrix composites were fabricated by spark plasma sintering (SPS) by a D. R. Sinter® SPS3.20 (Sumitomo Coal & Mining, now SPS Syntex Inc.). Besides, the sintering process was accomplished at protective Ar environment, a pressure of 40 MPa and 1150 °C for 10 min. The as prepared samples were polished using emery papers with 1200 grits and then with 0.05 μm wet polishing diamond pastes up to a mirror finish.

NiAl alloy without GNPs and silver was denoted as NA. While NAS, NAG, NAGS10 and NAGS15 represented NiAl matrix composites with 10 wt% silver, 1.5 wt% GNPs, 1.5 wt% GNPs-10 wt% silver and 1.5 wt% GNPs-15 wt% silver, respectively.

The surface hardness of the samples was measured 6 times at each side and the average values were taken using HVS-1000 Vickers's hardness instrument with a load of 1 kg and 8 seconds of dwell time according to the standards.[24] Furthermore, the densities of the samples were measured based on Archimedes principles and according to the ASTM Standard B962-08.[25]

The microstructure of the contact worn surfaces and the cross sections of the worn surfaces were examined using electron probe microanalysis (EPMA, JAX-8230), field emission scanning electron microscope (FESEM, ZEISS ULTRA PLUS) and energy dispersive spectroscopy (EDS, Inca X-Act). In addition, the chemical composition and phases of the samples were examined by X-ray diffraction (XRD) test using CuKα radiation at 30 kV and 40 mA at a scanning speed of 0.01° s^{-1}.

2.2 Tribological tests

The frictional characteristics of NA, NAG, NAGS10 and NAGS15 were tested on HT-1000 ball on disc high temperature tribometer according to the ASTM Standard G99-95.[26] The disk was the samples and the counterpart ball was the commercial Si_3N_4 ceramic ball with a diameter of 2 mm (about HV 15 ± 0.5 GPa) as shown in Fig. 1. Moreover, the contact surfaces were cleaned by acetone and dried using hot air to get rid of the dirt and any other phase of contaminants.

The worn volume was calculated based on the following formula:

$$\text{Worn volume } (V) = A \times L \quad (1)$$

where V is the volume worn away in (mm^3), and it was determined by the profiles of the worn scar cross-section measured using a surface profile meter.

The wear results of the samples after the friction process have been presented as a specific wear rate, and it can be calculated according the formula presented as follow:

$$\text{Specific wear rate} = V/(P \times L) \quad (2)$$

where, P is the load in N and L is the sliding distance in m.

The tribological tests were performed under different conditions of sliding velocities (0.2, 0.4, 0.6 and 0.8 m s^{-1}) and applied loads (3, 6, 9 and 12 N). The sliding time was exactly 20 minutes. Moreover, the humidity at the surrounding environment was 65% at all tests.

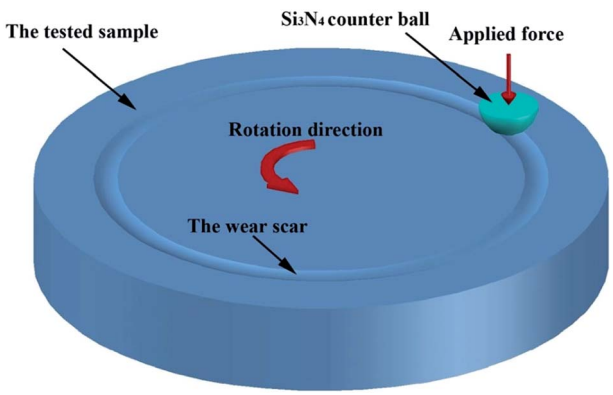

Fig. 1 Schematic view of pin on disc tribometer.

3. Results and discussions

3.1 Material composition, hardness and densities

Fig. 2 shows the XRD patterns of NAG, NAGS10 and NAGS15 composites. It is clear that all the composites mainly consist of NiAl phase. Meanwhile, the carbon could be noticed at 30° of diffraction angle. Moreover, the silver was presented in NAGS10 and NAGS15 composites at angles of 45° and 55°.

The chemical compositions, microhardness and densities of NA, NAG, NAGS10 and NAGS15 are shown in Table 1. The measured values of micro hardness and densities reveal that the increase in silver content can lead to an increase in the densities of samples. Meanwhile, the micro hardness decreases with the increase of the silver percentage. Also, it could be observed that the micro hardness of NiAl composites increase for the addition of GNPs.

3.2 Friction behavior and wear mechanism

Fig. 3 shows the effect of sliding speeds on the friction coefficients and wear rates of NA, NAS, NAG, NAGS10 and NAGS15 composites under normal load of 12 N and room temperature. It can be noticed that NA exhibits the highest friction coefficients and wear rates among all composites at different sliding speeds. Also, it can be observed that the friction coefficient of NAG composites decrease after 0.4 m s^{-1} of sliding speed. This behavior is attributed to the adhesion behavior of NiAl, which is high under low sliding velocity. In addition, the graphene layer deteriorates by tearing rather than shearing at sliding velocities below 0.6 m s^{-1}.[1] NAS composites show lower friction coefficient than NAG composites at low sliding speeds. The friction coefficient of NAGS10 composites increase with the increase of the sliding velocity and reach to 0.26 at 0.4 m s^{-1}. It tends to decrease at 0.6–0.8 m s^{-1} of sliding velocities and reaches to the minimum value of 0.16 at 0.8 m s^{-1}. NAGS15 composites exhibit low friction coefficients at high sliding speeds, while the wear rates increase as the sliding velocity increases up to 0.6 m s^{-1}, then it begins to decrease. Therefore, NAGS10 composites exhibit the best tribological properties. It is observed that adding 1.5 wt% graphene and 10 wt% Ag could decrease the friction coefficients of NAGS10 by 77.55, 26.5 and 20.92%, if compared to NA, NAG and NAS composites.

As shown in Fig. 3(b), the wear resistance is also significantly affected by the combined lubricants. It is observed that the wear resistance of NAGS10 is the highest among all composites at different sliding velocities. The wear resistance of NAGS10 composites decreases with the increase of the sliding speed. Moreover, the minimum value was recorded 3.19×10^{-6} mm^3 N^{-1} m^{-1} at 0.2 m s^{-1}. Adding 1.5 wt% graphene and 10 wt% silver could improve the wear resistance of NAGS10 by 99.3, 62.28 and 36.3%, if compared to NA, NAS and NAG composites. This behavior may be related to the formation of silver islands during SPS process, which provides a low shearing resistance of the surface layer.

Fig. 4 shows the elements distribution of NAGS10 composites. It is clear that the silver and the GNPs are present in the sample surface. It can be also seen that Ni, Al, Cr, Nb, C and Mo are present in the composites. Besides, it could be observed that the silver could diffuse over the sample surface to form separate islands which contain GNPs. This typical behavior of silver diffusion has been investigated in previous study.[27] It is reported that the presence of silver in YSZ–Ag–Mo coatings protect the inside coating from oxidation through the diffusion and coalescence over the surface.

The formation mechanism of the lubrication film is shown schematically in Fig. 5. Due to the heating during SPS process, the silver particles which exist on the subsurface layer rise to the surface through the voids between the particles of the other materials. Then, separate silver islands begin to be formed on the surface of the samples and some of these islands could contain GNPs as shown in Fig. 5(b). During the sliding process, those islands are deformed and spread out over the surface to form a coalescence layer in some areas on the sample surface as shown in Fig. 5(c). For further understanding of the lubrication

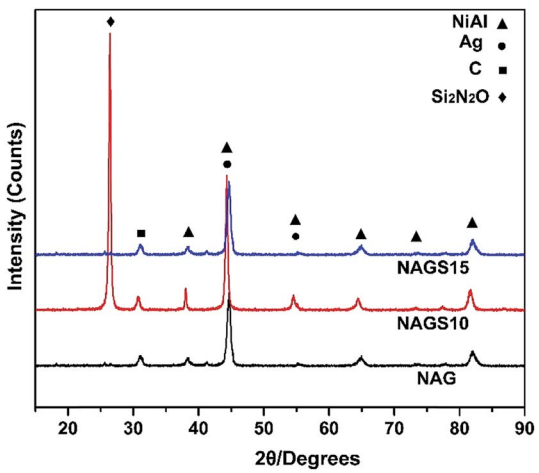

Fig. 2 XRD patterns of NAG, NAGS10 and NAGS15 composites after sliding tests at 3 N and 0.2 m s^{-1}.

Table 1 The composition, hardness and density of the composites

Sample	Composition (wt%)	Microhardness (GPa)	Density (gm cm^{-3})
NA	NiAl	5.54	5.67
NAS	NiAl + 10 wt% silver	3.92	5.89
NAG	NiAl + 1.5 wt% graphene	5.68	5.21
NAGS10	NiAl + 1.5 wt% graphene + 10 wt% silver	4.94	5.45
NAGS15	NiAl + 1.5 wt% graphene + 15 wt% silver	4.24	5.53

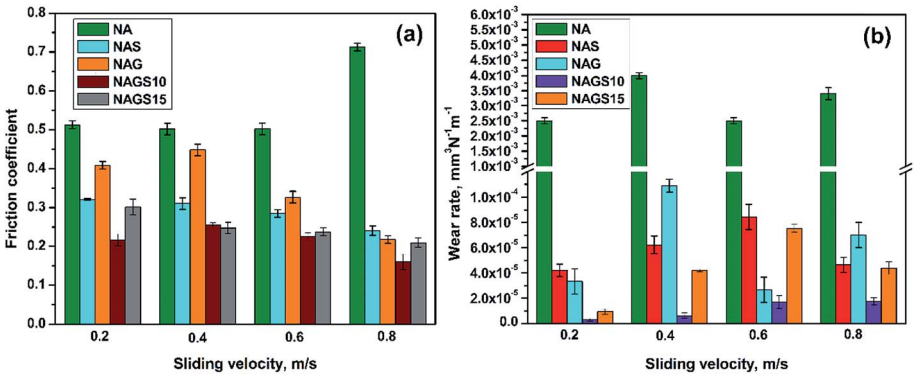

Fig. 3 The average friction coefficients (a) and wear rates (b) of NA, NAS, NAG, NAGS10 and NAGS15 at different sliding speeds.

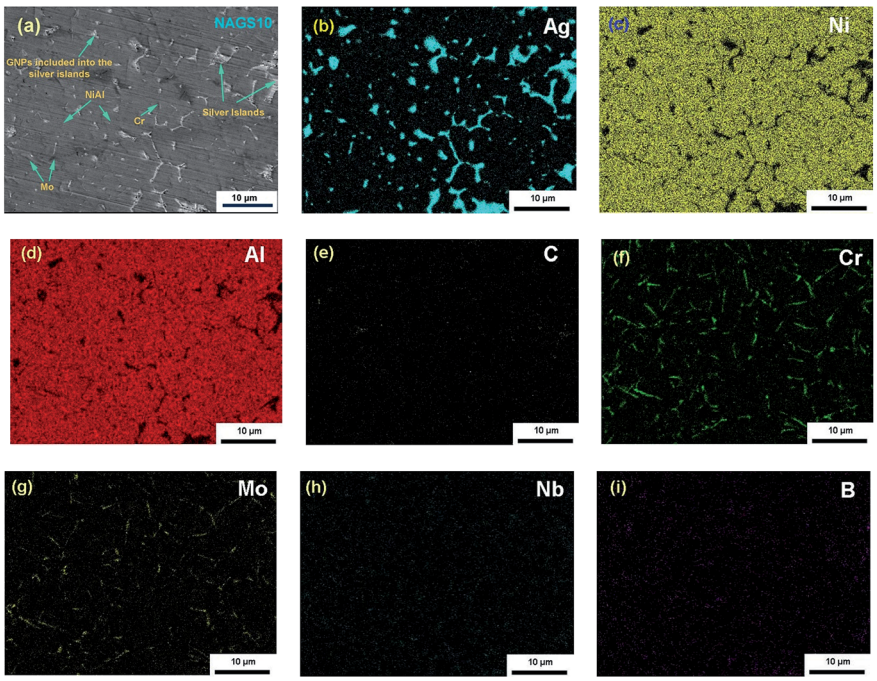

Fig. 4 The elements distributions of NAGS10 composites.

mechanism, the wear tracks morphologies of NAG, NAS, NAGS10 and NAGS15 composites were tested as shown in Fig. 6.

It is observed that surface layers of NAG composites are delaminated due to the high adhesion of NiAl matrix composites at low sliding speed as proved in previous studies.[1] Smoother surface, deep surface cracks and graphene free silver islands could be seen on the wear track of NAS composites as shown in Fig. 6(b). Those islands could lead to a decrease in the friction coefficient, if compared to NA and NAG composites. However, the deep surface cracks could increase the wear rates of NAS when compared with NAGS10 and NAGS15 composites. However, groups of graphene–silver islands and smoother surfaces could be seen on the wear track of NAGS10 composites as shown in Fig. 6(c). The silver layer acts as an intermediate layer between the NiAl substrate and the GNPs, which can ease the shearing of the surface layer significantly. The silver islands act as the bearing areas that play the major role in load transition. Furthermore, the silver layer containing GNPs provides a low conjunction layer, leading to stresses dissipation and easing the slipping of the layers of the GNPs on the surface layer.

The typical shearing mechanism of NAGS10 and NAGS15 are shown in Fig. 7. The GNPs are directly attached to the NiAl substrate in NAG composites. In contrast, the GNPs are attached to silver layer which is softer than NiAl substrate. During the sliding, NAGS10 and NAGS15 exhibit the lower friction coefficients than NAG composites due to the further relative slippage between the graphene layer and the silver layer, and this lubrication mechanism decreases the shearing forces significantly, leading to the decrease in the friction forces. The increase in the silver content up to 15 wt% leads to an increase in the friction coefficient for NAGS15, if compared to NAGS10

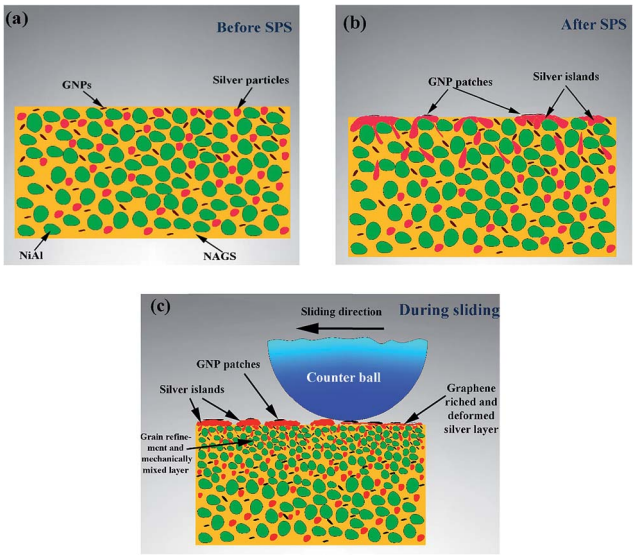

Fig. 5 Schematic diagram of formation of the lubrication film of NAGS10 and NAGS15 composites, before SPS (a), after SPS (b) and during sliding (c).

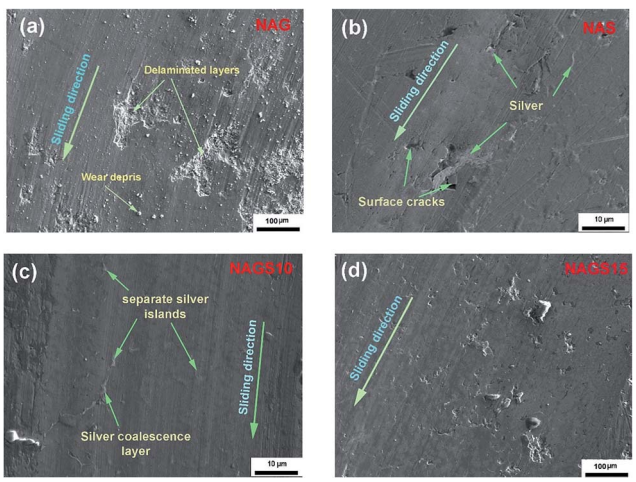

Fig. 6 SEI images of wear tracks of NAG (a), NAS (b), NAGS10 (c) and NAGS15 (d) at RT, 12 N and 0.2 m s^{-1} of sliding speed.

composites. This behavior may be attributed to that the increase in silver content may lead to an increase of the graphene free-silver islands, resulting in an increase of shearing forces, thus causing the increase of the friction coefficient. On the other hand, the effect of number of layers and the thickness of the layer of GNPs on the friction coefficient could be observed in the nano scale so they have a limited effect in micro scale testing.[28,29]

The formation of the GNPs silver island leads to a sharp increase in the wear resistance of NAGS10 composites. This behavior could be interpreted as the graphene–silver islands are able to slip for long distances without tearing which lead to free cracks surfaces as shown in Fig. 6(b). Furthermore, the presence of silver decreases the tendency of the adhesion between the

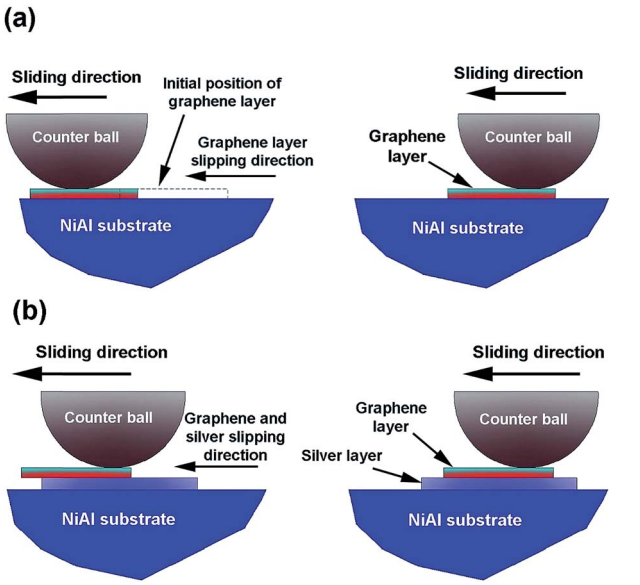

Fig. 7 Schematic diagram of the shearing mechanism of NAG composites (a), NAGS10 and NAGS15 (b) during the sliding process.

NAGS10 composites and the counter ball. Consequently, the wear rates decreases sharply.

Fig. 8 shows the morphologies of the worn surfaces of the NAGS10 and NAGS15 composites at sliding speed range from 0.4–0.8 m s^{-1}. A highly deformed surface layer could be seen on the surface of the NAGS10 and NAGS15 composites at 0.4 m s^{-1} of sliding speed. In addition, a micro cutting could be observed

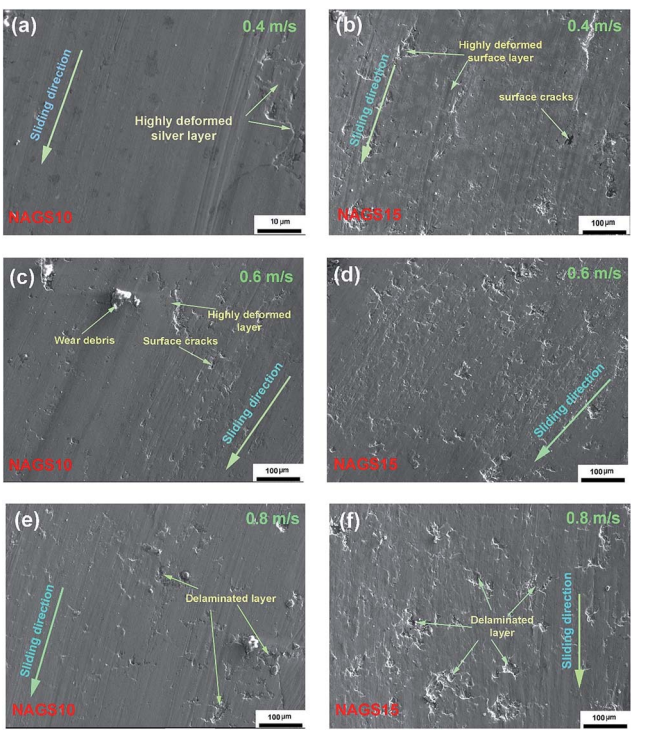

Fig. 8 SEI images of NAGS10 and NAGS15 composites at different sliding velocities and 12 N of applied load.

on the surface of NAGS10 composites. Meanwhile, shallow surface layer delamination could be observed on the surface of NAGS15 composites at the same sliding velocity. In contrast, smoother surfaces of NAGS10 and NAGS15 composites could be noticed at 0.2 m s^{-1} of sliding speed as shown in Fig. 6(b) and (c).

The shearing stresses increase with the increase of the sliding velocity, resulting in the failure of the surface layer due to the severe plastic deformation. As a result of the excessive plastic deformation, small surface cracks tend to appear on the NAGS10 surface at sliding velocity of 0.6 m s^{-1}. At the same time, the surface cracks and delamination increase with the increase of sliding velocity, leading to an increase in the wear rate of NAGS15 composites. The wear mechanism changes from micro cutting to a typical fatigue mechanism as the sliding velocity increases up to 0.8 m s^{-1}. Delaminated layers are seen on the NAGS10 surfaces as shown in Fig. 8(e). The delaminated layers of NAGS15 composites increase as the sliding velocity increases up to 0.8 m s^{-1}. Nevertheless, these delaminated layers are shallower than those created at sliding speed of 0.6 m s^{-1}, resulting in a slight decrease in the wear rate. For further understanding of the characteristics of the surface layer, FESEM tests were performed on the cross sections of the worn surfaces. It could be observed that silver–GNPs enriched thin separate deformed layers are formed on the surface of NAGS10 composites after the sliding process as shown in Fig. 9(a). The formation of those layers lead to a further improvement in the friction coefficients and wear resistance as discussed before. However, a thick continuous silver layer is formed on the surface of NAGS15 composites. These thick layers containing silver and small amount of GNPs exhibit higher friction coefficients and wear rates as a result of decreasing the GNPs percentage in the silver layer, if compared to NAGS10 composites.

Due to the excellent tribological characteristics of NAG10 composites at different sliding velocities, it was required to explore the frictional characteristics and the wear resistance of NAGS10 during sliding under different loads.

Fig. 10 shows the friction and wear behaviors at different applied loads. It is clear that the friction coefficient decreases with the decrease of the applied load and reaches to the minimum value of 0.11 at 12 N. While, the wear rate decreases to 1.7×10^{-5} mm^3 N^{-1} m^{-1} as the load increases up to 9 N, then it slightly increase at 12 N. For exploring the wear mechanisms of NAGS10 composite at different applied loads, EPMA tests for the worn surfaces were done.

As shown in Fig. 11(a), the wear mechanism of NAGS10 at 3 N is typically adhesion mechanism. Groups of delaminated layers can be seen on the surface of NAGS10 composites at applied load of 3 N, in addition the worn surface contains the wear debris and the counter ball remains in the form of Si_2N_2O as a result of the adhesion between the sample and the Si_3N_4 counter ball which is proved by XRD results and SEI images shown in Fig. 2 and 11(a). The adhesion between the counter ball and the sample decreases as the applied load increases and the wear mechanism become a mixed mechanism between adhesion and micro ploughing, hence the new wear mechanism leads to a significant decrease in friction coefficient and wear rate as shown in Fig. 11(b). The compaction of the wear debris is also a rational reason of decreasing the friction coefficient of NAGS10 at 6 N whereas the accumulated stresses and the rise of the temperature caused by the friction process at higher loads could ease the compaction of the wear debris which leave relative smooth surfaces. Moreover, the existence of GNPs–silver islands decreases the adhesion between the counter ball and sample significantly which led to a remarkable improvement of the tribological characteristics of NAGS10 at loads higher than 6 N. Fig.11(c) shows the worn surface of NAGS10 at 9 N of applied load. It is clear that the silver–GNPs islands became more effective at load of 9 N. Meanwhile, the silver–

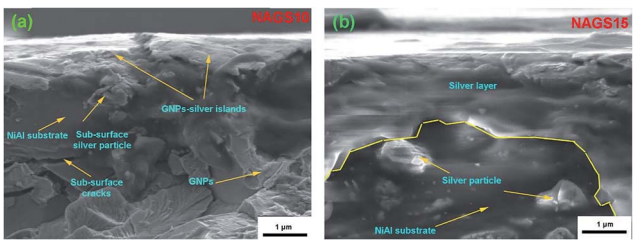

Fig. 9 FESEM images of NAGS10 (a) and NAGS15 (b) composites at 0.8 m s^{-1} of sliding velocity and 12 N of applied load.

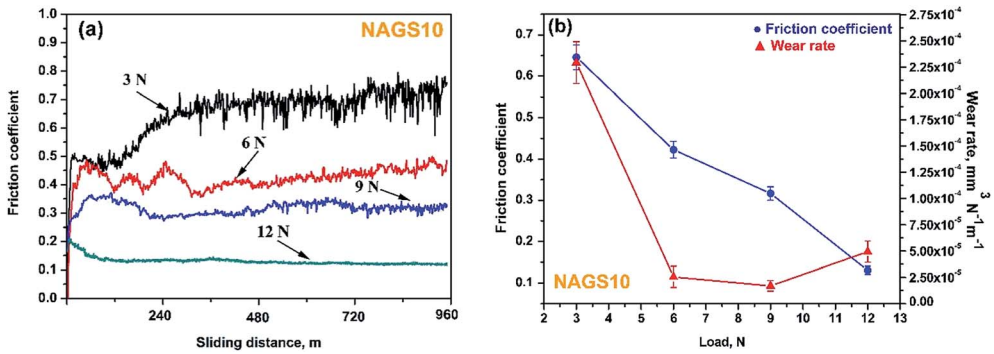

Fig. 10 Friction coefficient variation (a), the average wear rate and the average friction coefficients (b), for NAGS10 at RT and 0.2 m s^{-1} of sliding speed.

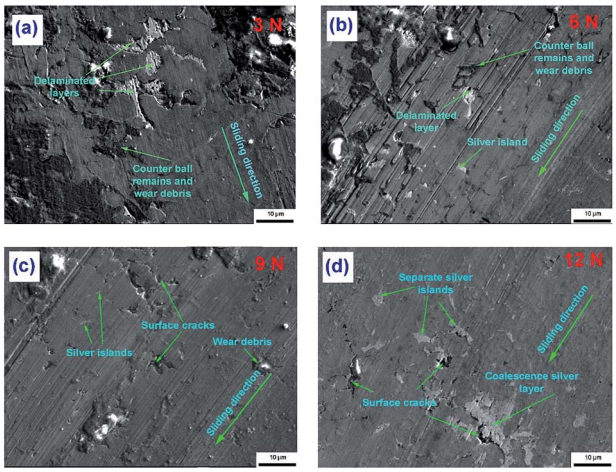

Fig. 11 EPMA images of the worn surfaces of NAGS10 at 3 N (a), 6 N (b), 9 N (c) and 12 N (d) at sliding speed of 0.2 m s^{-1}.

GNPs enriched compacted wear debris act as a lubrication phase and lead to a decrease in the friction coefficient and wear rate of NAGS10 composites. The silver islands became highly deformed due to the high accumulated stress at applied load of 12 N. The excessive plastic deformation of those islands and the worn surface of the NAGS10 composites leads to a further decrease in the coefficient of friction, while the surface and subsurface cracks tend to appear causing an increase in the wear rate as shown in Fig. 9(a) and 11(d).

4. Conclusions

This article presents a comprehensive study of using hybrid lubrication effect of silver and GNPs based on the tribological and microstructure tests. It is also gives a comparative study of the tribological properties of NA, NAS, NAG, NAGS10 and NAGS15 composites prepared by SPS technique. Moreover, the beneficial role of the combined lubricants has been investigated. It was concluded that adding GNPs and silver could improve the tribological properties of NiAl composites significantly. NAGS10 shows the best tribological properties at different sliding velocities among whole composites, where the minimum coefficient of friction is recorded as 0.16 at 0.8 m s^{-1} of sliding speed. While the minimum wear rate is 3.19 × 10^{-6} mm^3 N^{-1} m^{-1} at 0.2 m s^{-1}. This behavior is attributed to that the formation of GNPs–silver enriched islands eases the slipping of the graphene sheets over the NiAl substrate and acts as a bearing areas playing the major role in force transition and stresses dissipation. Increasing the silver content up to 15 wt% leads to a slight increase in the friction coefficient and wear rate. It is also observed that NAGS10 shows the minimum wear rate at load of 9 N as a result of the change of the wear mechanism. While the friction coefficient is 0.13 at 12 N of applied load due to the presence of the GNPs–silver island and the compacted wear debris which act as a lubricant.

Acknowledgements

This work was supported by the Project for Science and Technology Plan of Wuhan City (2013010501010139) and the National Natural Science Foundation of China (51275370). The authors also wish to gratefully thank the Material Research and Testing Center of Wuhan University of Technology for their assistance.

References

1 A. M. M. Ibrahim, X. L. Shi, W. Z. Zhai, J. Yao, Z. S. Xu, L. Cheng, Q. S. Zhu, Y. C. Xiao, Q. X. Zhang and Z. H. Wang, *Tribol. Trans.*, 2014, **57**, 1044–1050.
2 D. Miracle, *Acta Mater.*, 1993, **41**, 649–684.
3 J. T. Guo, *Ordered Intermetallic Compound NiAl Alloy*, Science Press, Beijing, 2003, p. 58.
4 M. T. Guo and C. Y. Tsao, *Mater. Sci. Eng., A*, 2002, **333**, 134–145.
5 B. Chen, Q. Bi, J. Yang, Y. Xia and J. Hao, *Tribol. Int.*, 2008, **41**, 1145–1152.
6 P. Rohatgi, S. Ray and Y. Liu, *Int. Mater. Rev.*, 1992, **37**, 129–152.
7 D. Berman, A. Erdemir and A. V. Sumant, *Mater. Today*, 2014, **17**, 31–42.
8 M. Belmonte, C. Ramírez, J. González-Julián, J. Schneider, P. Miranzo and M. I. Osendi, *Carbon*, 2013, **61**, 431–435.
9 A. Nieto, D. Lahiri and A. Agarwal, *Carbon*, 2012, **50**, 4068–4077.
10 M. J. Nine, M. A. Cole, D. N. Tran and D. Losic, *J. Mater. Chem. A*, 2015, **3**, 12580–12602.
11 X. An and C. Y. Jimmy, *RSC Adv.*, 2011, **1**, 1426–1434.
12 D. Marchetto, C. Held, F. Hausen, F. Wählisch, M. Dienwiebel and R. Bennewitz, *Tribol. Lett.*, 2012, **48**, 77–82.
13 W. Z. Zhai, X. L. Shi, M. Wang, Z. S. Xu, J. Yao, S. Y. Song and Y. F. Wang, *Wear*, 2014, **310**, 33–40.
14 D. Lahiri, F. Hec, M. Thiesse, A. Durygin, C. Zhang and A. Agarwal, *Tribol. Int.*, 2014, **70**, 165–169.
15 W. Z. Zhai, X. L. Shi, J. Yao, A. M. M. Ibrahim, Z. S. Xu, Q. S. Zhu, Y. C. Xiao, L. Chen and Q. X. Zhang, *Composites, Part B*, 2015, **70**, 149–155.
16 K. Yang, X. L. Shi, W. Z. Zhai, L. Chen, A. Zhang and Q. X. Zhang, *RSC Adv.*, 2015, **5**, 44618–44625.
17 E. Kuk, G. Kim and C. Lee, *J. Ceram. Process. Res.*, 2005, **6**, 95.
18 R. Tyagi, D. S. Xiong, J. Li and J. Dai, *Wear*, 2010, **269**, 884–890.
19 R. Tyagi, D. Xiong and J. Li, *Wear*, 2011, **270**, 423–430.
20 E. Y. Liu, W. Z. Wang, Y. M. Gao and J. H. Jia, *Tribol. Int.*, 2013, **57**, 235–241.
21 J. Yao, X. L. Shi, W. Z. Zhai, A. M. M. Ibrahim, Z. S. Xu, S. Y. Song, L. Chen, Q. S. Zhu, Y. C. Xiao and Q. X. Zhang, *J. Mater. Eng. Perform.*, 2015, **24**, 307–318.
22 X. L. Shi, J. Yao, Z. S. Xu, W. Z. Zhai, S. Y. Song, M. Wang and Q. X. Zhang, *Mater. Des.*, 2014, **53**, 620–633.
23 S. Zhu, F. Li, J. Ma, J. Cheng, B. Yin, J. Yang, Z. Qiao and W. Liu, *Tribol. Int.*, 2015, **84**, 118–123.

24 ASTM E92-82, *Standard Test Method for Vickers Hardness of Metallic Materials*, ASTM Int, 2003.
25 ASTM B962-08, *Standard Test Methods for Density of Compacted or Sintered Powder Metallurgy (PM) Products Using Archimedes' Principle*, ASTM Int, 2008.
26 ASTM G99-95, *Standard test method for wear testing with a pin on disk apparatus*, ASTM Int, 1995.
27 J. Hu, C. Muratore and A. Voevodin, *Compos. Sci. Technol.*, 2007, **67**, 336–347.
28 L. Xu, T.-B. Ma, Y.-Z. Hu and H. Wang, *Nanotechnology*, 2011, **22**, 285708.
29 C. Lee, Q. Li, W. Kalb, X.-Z. Liu, H. Berger, R. W. Carpick and J. Hone, *Science*, 2010, **328**, 76–80.